COMPARISON OF FINITE-DIFFERENCE SEISMOGRAMS AND RAY-THEORY TRAVEL TIMES IN THE ELASTIC SEG/EAGE SALT MODEL

VÁCLAV BUCHA

Department of Geophysics, Faculty of Mathematics and Physics, Charles University, Ke Karlovu 3, 121 16 Praha 2, Czech Republic. bucha@seis.karlov.mff.cuni.cz

ABSTRACT

Finite-difference seismograms for a selected shot and five receiver configurations computed in the elastic SEG/EAGE Salt Model during the Next-Generation Seismic Modelling and Imaging project are compared with ray-theory travel times. Two-point rays and travel times of direct, refracted and reflected P-waves and converted S-waves in the smoothed elastic SEG/EAGE Salt Model are computed.

KEY WORDS

Ray tracing, seismic waves, seismograms, travel times

INTRODUCTION

The original acoustic SEG/EAGE Salt Model contains P-wave velocity values (Aminzadeh *et al.*, 1997). House *et al.* (2004) calculated finite-difference seismograms in an elastic SEG/EAGE Salt Model. This elastic velocity model was supplemented by values of S-wave velocities and densities derived from the original P-wave velocity values. Elastic wave calculations were carried out using the modelling program called "E3D" (Larsen and Grieger, 1998). E3D is a finite-difference modelling code (4th order accurate in space, and 2nd order in time).

House *et al.* (2004) performed elastic numerical calculations within the Next-Generation Seismic Modelling and Imaging Project. The project started in 2000, as a collaboration among 20 industrial companies, two US national laboratories (Los Alamos National Laboratory and Lawrence National Laboratory), two universities (Stanford University and the University of Houston), and the modelling subcommittee of the SEG Research Committee. SEGY synthetic seismograms computed within Phase 1 finite-difference calculations in the elastic SEG/EAGE model are available via the internet (http://www.ees11.lanl.gov/projects/next-gen).

We compare finite-difference seismograms and ray-theory travel times for shot number 145 and five receiver configurations. Three configurations are simulated marine streamer surveys running in three directions: East, South, West. Two configurations are simulated ocean-bottom cables with cables aligned North-South and East-West. The smoothed SEG/EAGE Salt Model (Bulant, 2001, 2002, 2004) was supplemented by S-waves and densities according to House *et al.* (2000).

The GOCAD program was used to visualize the 3-D smoothed Salt Model interfaces, shot, receiver lines and computed two-point rays. All computations were performed on a PC with the Linux operating system.

ELASTIC SMOOTHED SEG/EAGE SALT MODEL

The Salt Model selected for ray tracing computations was smoothed by Bulant (2001, 2002, 2004). It is the best model obtained as a result of many test smoothing computations. The model is parameterized by B-splines and was smoothed using Sobolev scalar products. The smoothed Salt Model is composed of the most important interfaces and velocity blocks. The interfaces, which are characterized by the highest discontinuities in the velocity field, are the ocean bottom, the interfaces limiting the salt body, the geopressure horizon and the bottom flat interface (see Figure 1). The velocity blocks are the water (velocity is constant), the background above the geopressure horizon (three-dimensionally varying velocity), the salt (velocity is constant), the background below the geopressure horizon (three-dimensionally varying velocity) and the bottom half-space (velocity is constant).

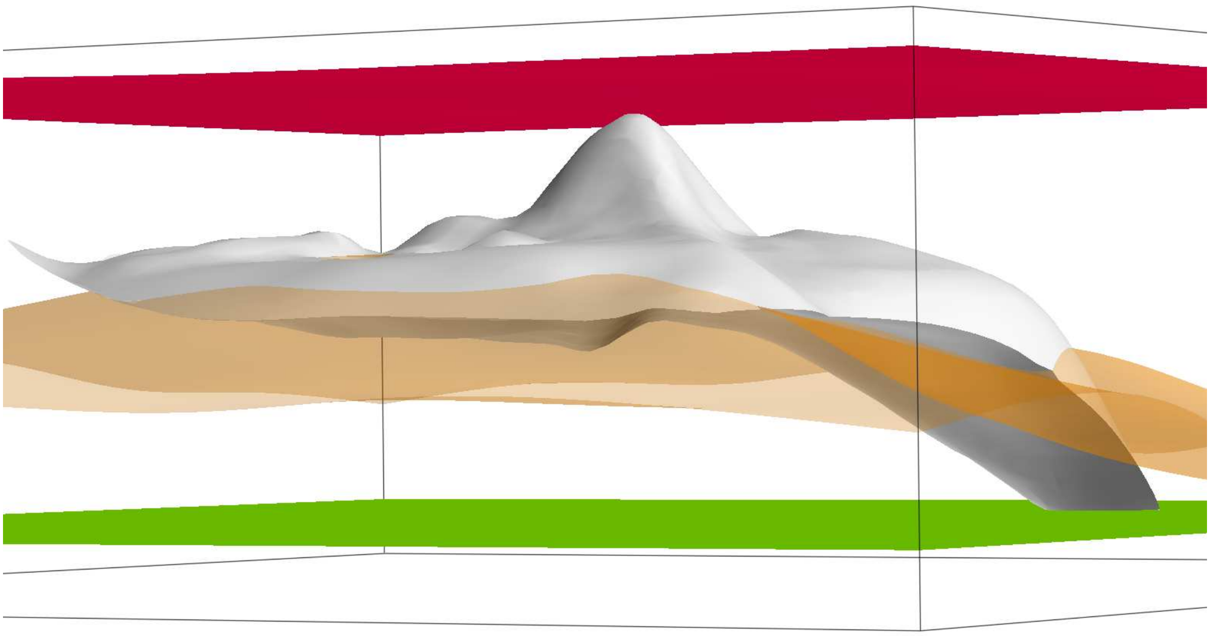

Figure 1. Detailed view of the salt body in the smoothed Salt Model. The most important interfaces are: the ocean bottom, the interfaces limiting the salt body, the geopressure horizon, the bottom flat interface. The geopressure horizon is partially transparent.

The smoothed acoustic SEG/EAGE Salt Model was supplemented by S-waves and densities according to House *et al.* (2000). S-wave velocities were derived from the smoothed P-wave velocities, ratio V_p/V_s being piecewise linearly dependent on depth (Table 1).

The densities in sediments were derived from P-wave velocities using the Gardner relation (Gardner *et al.*, 1974),

$$\varrho = 0.23 * (V_p)^{1/4} \quad ,$$

where ϱ is the density (g/cm^3) and V_p is the P-wave velocity (Ft/s). A constant density of 2.2 g/cm^3 was used for salt.

Depth (km)	V_p/V_s
Water (all depths)	∞ ($V_s = 0.0$)
0.0 sediments	5.0
0.6	3.5
1.5	3.0
3.0	2.5
4.5	2.3
6.0	2.0
Salt (all depths)	1.9

Table 1. V_p/V_s values that approximate the velocity depth trend appropriate for the Gulf of Mexico.

SOURCE AND RECEIVERS

Ray tracing computations were performed for one shot common to five receiver configurations, marine streamers and ocean bottom cables. In the Next Generation Seismic Modelling and Imaging Project, Phase 1, a 17 by 17 grid of shot locations was defined, with a shot spacing of 480 m (House *et al.*, 2004). The grid of shots covered almost the entire salt body of the SEG/EAGE model. We have selected shot number 145 located at the centre of the grid.

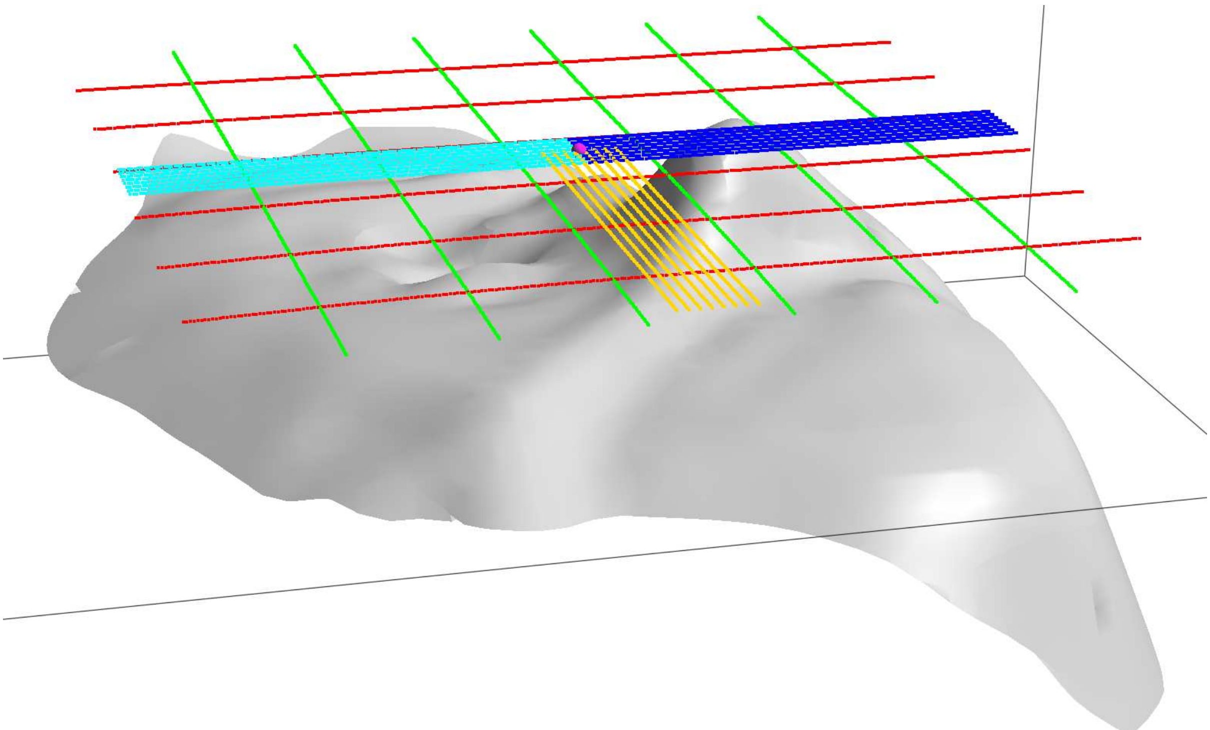

Figure 2. Perspective view of the shot, five receiver configurations and the salt body.

Figures 2 and 3 show the location of the selected shot and five receiver configurations above the salt body. The shot (magenta sphere) is located in the ocean at a depth of 12m. The three sets of eight lines starting at the shot location represent marine streamer

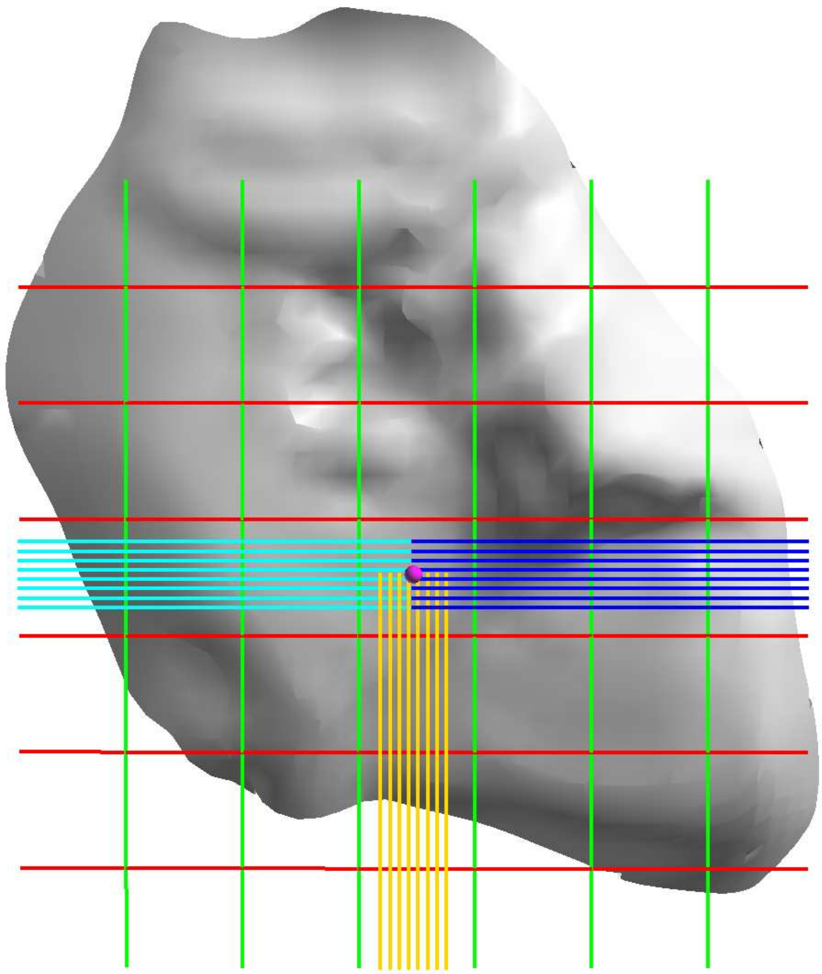

Figure 3. Top view of the shot, five receiver configurations and the salt body.

surveys running East (blue lines), South (yellow lines) and West (cyan lines). Each line consists of 141 groups of one-component hydrophones with a group interval of 24m. Hydrophones are located at a depth of 12m.

There are two four-component ocean bottom cable configurations, one running North-South (six green lines) and one East-West (six red lines). Each line consists of 281 groups with a group interval of 24m. Each receiver group contains a hydrophone as well as a three-component set of geophones (House *et al.*, 2000).

RAY TRACING COMPUTATIONS

The two-point rays and travel times in the elastic smoothed SEG/EAGE Salt Model were computed using the MODEL, CRT and FORMS subroutine packages (Červený *et al.*, 1988; Bucha and Bulant, 2006). The most time-consuming step of the calculation is the two-point ray tracing. Ray tracing output files are then converted to travel times. The two-point rays of the computed waves, shot and receivers are added to the GOCAD files. A more detailed description of the computation steps can be found in Bucha (2005, 2006).

MARINE STREAMER CONFIGURATIONS

Two-point rays of 24 elementary waves were calculated for each line of three simulations of the marine streamer survey in the East, South and West direction.

(1) 18 elementary P-waves: direct wave, wave refracted under the ocean bottom, wave refracted in the salt body, 1x, 2x, 3x, 5x, 10x reflected from the ocean bottom, combinations of waves refracted under the ocean bottom and reflected from the ocean bottom, wave reflected 1x and 2x from the top of salt body, wave reflected from the bottom of the salt body, wave reflected from the bottom interface.

(2) 6 elementary P-waves converted to S-waves and back to P-waves: P-wave reflected and converted to S-wave at the top of the salt body, P-wave refracted and converted to S-wave in the salt body, P-wave reflected and converted to S-wave at the bottom of the salt body, P-wave converted to S-wave at the top of the salt body and reflected from the bottom of the salt body, P-wave converted to S-wave at the ocean bottom and reflected from the top of the salt body, P-wave converted to S-wave at the ocean bottom and reflected from the bottom of the salt body.

The top interface (sea level) at the depth of 0m is used for storing computed quantities. Receivers are at depths of 12m, and travel times are interpolated from the top interface.

OCEAN BOTTOM CABLE CONFIGURATIONS

Two-point rays of 30 elementary waves were calculated for each line of two simulations of ocean bottom cable survey in the North-South and East-West direction.

(1) During the computations of the direct P-wave some of the rays were tangent to the weakly curved ocean bottom surface and the computation crashed. The receivers are positioned at the ocean bottom. It was necessary to add a reference surface near to the ocean bottom, and to project all receiver points onto the reference points "visible" to the rays. The travel times were extrapolated from the reference points to the receivers.

(2) 16 elementary waves were stored at the positive ("top") side of the ocean bottom surface. The last reflection before storing was from the sea level.

   (2a) 11 elementary P-waves: 1x, 2x, 4x, 9x reflected from the ocean bottom, combinations of waves refracted under the ocean bottom and reflected from the ocean bottom, wave reflected 1x and 2x from the top of salt body, wave reflected from the bottom of the salt body, wave reflected from the bottom interface.

   (2b) 5 elementary P-waves converted to S-waves and back to P-waves: P-wave reflected and converted to S-wave at the top of the salt body, P-wave reflected and converted to S-wave at the bottom of the salt body, P-wave converted to S-wave at the top of the salt body and reflected from the bottom of the salt body, P-wave converted to S-wave at the ocean bottom and reflected from the top of the salt body, P-wave converted to S-wave at the ocean bottom and reflected from the bottom of the salt body.

(3) 13 elementary waves were stored at the negative ("bottom") side of the ocean bottom surface.

(3a) 8 elementary P-waves: wave refracted under the ocean bottom, wave refracted in the salt body, combinations of waves refracted under the ocean bottom and reflected from the ocean bottom, wave reflected 1x and 2x from the top of salt body, wave reflected from the bottom of the salt body, wave reflected from the bottom interface.

(3b) 5 elementary P-waves converted to S-waves: P-wave reflected and converted to S-wave at the top of the salt body, P-wave reflected and converted to S-wave at the bottom of the salt body, P-wave converted to S-wave at the top of the salt body and reflected from the bottom of the salt body, P-wave converted to S-wave at the ocean bottom and reflected from the top of the salt body, P-wave converted to S-wave at the ocean bottom and reflected from the bottom of the salt body.

COMPARISON OF SEISMOGRAMS AND TRAVEL TIMES

Finite-difference seismograms were read and plotted using the Seismic Unix programs (Cohen and Stockwell, 2004). Plots of finite-difference seismograms correspond to the hydrophones for marine surveys and to the vertical component for the ocean bottom cable surveys. Shots are simulated by air-gun sources, and use a Ricker wavelet with a central frequency of 8Hz (House *et al.*, 2004). This frequency represents a compromise between frequency and the amount of computing time required. Seismograms are computed up to the 5th second.

Ray-theory travel times are calculated for three marine streamer configurations (24 receiver lines) and two ocean bottom cable configurations (12 receiver lines). Travel times are computed up to the 8th second but plotted only up to the 5th second for comparison with the finite-difference seismograms. Colour coded travel times of the individual elementary waves are plotted.

Figures 4 to 8 show the finite-difference seismograms, ray-theory travel times and two-point rays of five selected elementary waves. The ray-theory travel times are mostly denoted by the CalComp centred symbol $+$ and colour coded, but the travel time of the selected elementary wave is plotted with centred symbols $|$. The black $+$ denotes the direct wave, the wave refracted under the ocean bottom, and the wave refracted in the salt body, the red $+$ denotes multiple reflections from the ocean bottom, the green $+$ denotes combinations of waves refracted under the ocean bottom and reflected from the ocean bottom, the blue $+$ denotes multiple reflections from the top of the salt body, the yellow $+$ denotes the wave reflected from the bottom of the salt body, the cyan $+$ denotes the wave reflected from the bottom interface, the magenta $+$ denotes P-waves converted to S-waves.

Figures 4, 5 and 6 show finite-difference seismograms, ray-theory travel times generated from 24 elementary waves and two-point rays of a selected elementary wave for marine streamer surveys. Only one selected line for each direction (East, South and West) is plotted. The distance between the receiver lines in each streamer survey is 80m and the differences between seismograms in each streamer survey are small.

Figures 7 and 8 show finite-difference seismograms, ray-theory travel times generated from 30 computed elementary waves and two-point rays of a selected elementary wave for ocean bottom cables. Only one selected line for each direction (North-South and East-West) is plotted. For seismograms of other ocean bottom cable lines see Bucha (2006).

The comparison of finite-difference and ray-theory travel times in this paper shows differences. Some of the arrivals of elementary waves are clearly visible, some arrivals are not so clear or are shifted in time or position. The differences can be explained as follows:

- Ray-theory travel times are calculated in the smoothed elastic SEG/EAGE Salt Model,
- Application of the source time function, Ricker signal (FD arrival times differ from the travel times),
- Ray-theory travel times are computed for limited number of elementary waves.

A detailed comparison of finite-difference seismograms and travel times requires interactive displaying of rays of elementary waves. The ray paths are very complicated for some waves.

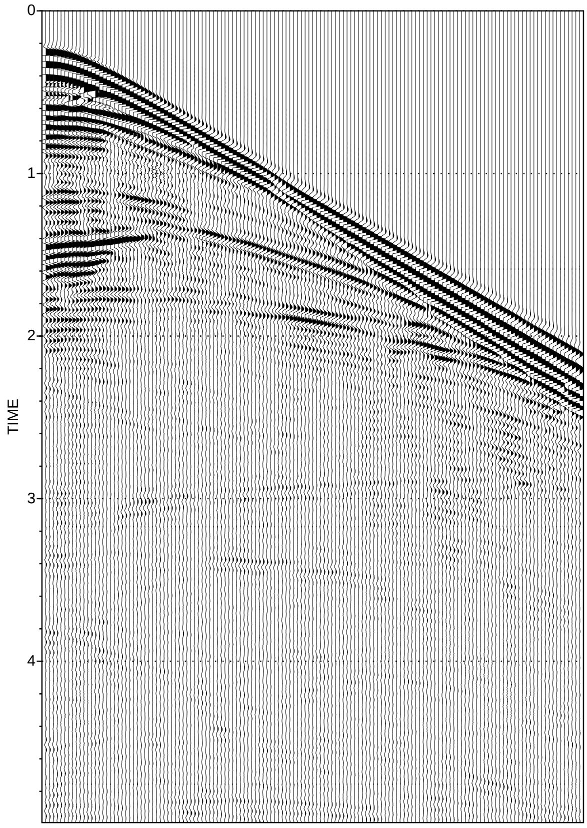

Finite-difference seismograms

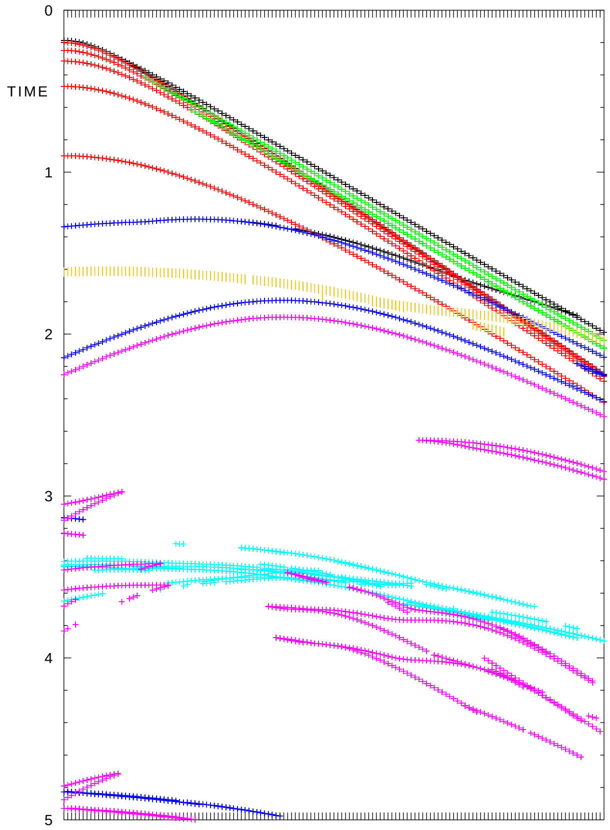

Ray-theory travel times

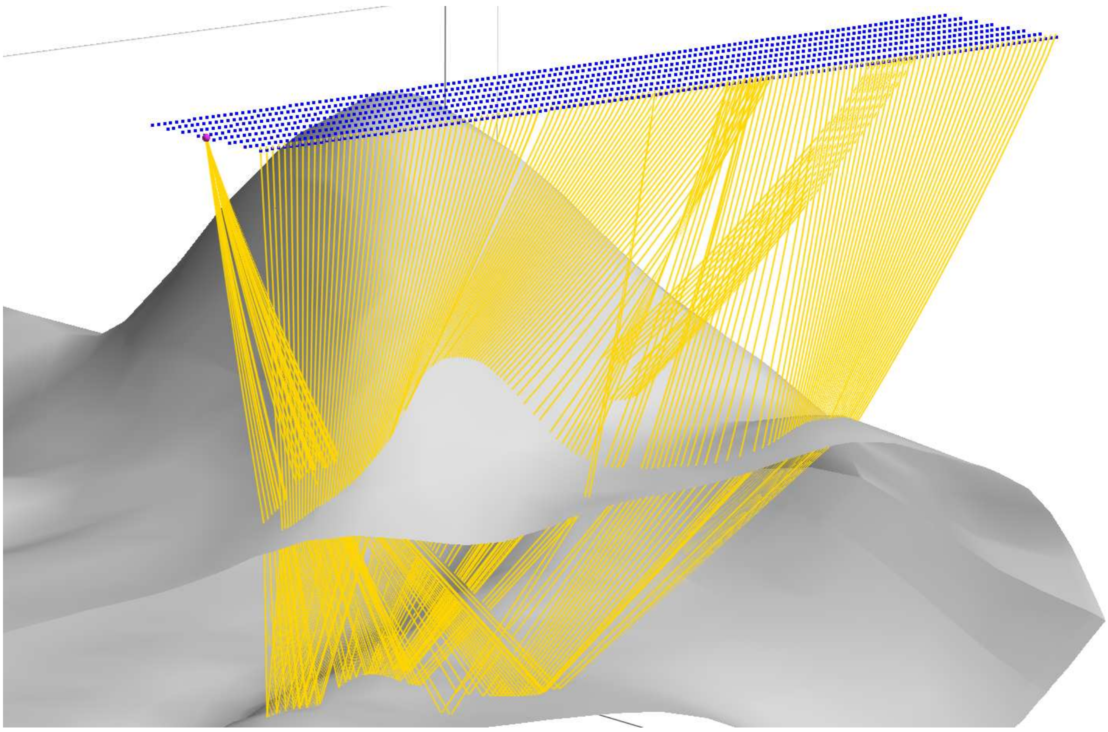

Rays of P-wave reflected from the bottom salt interface.

Figure 4. Marine streamer, East direction, line 1.

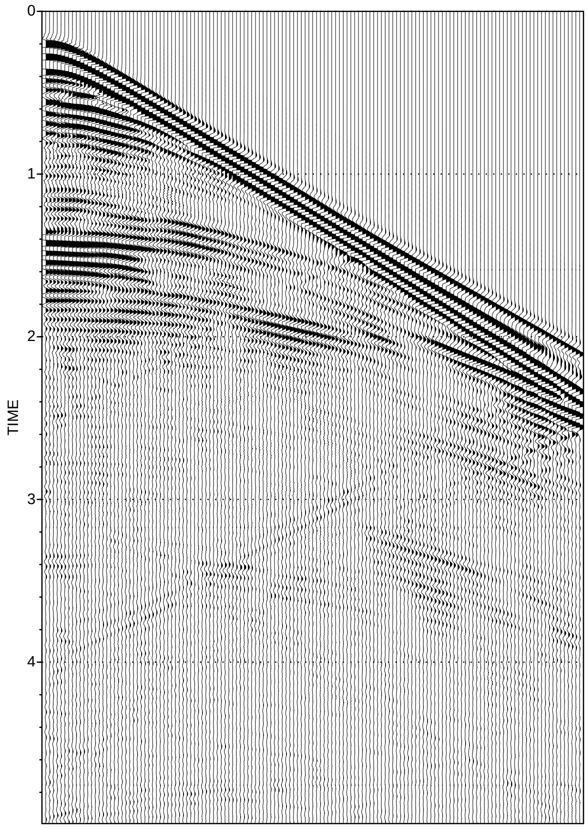

Finite-difference seismograms

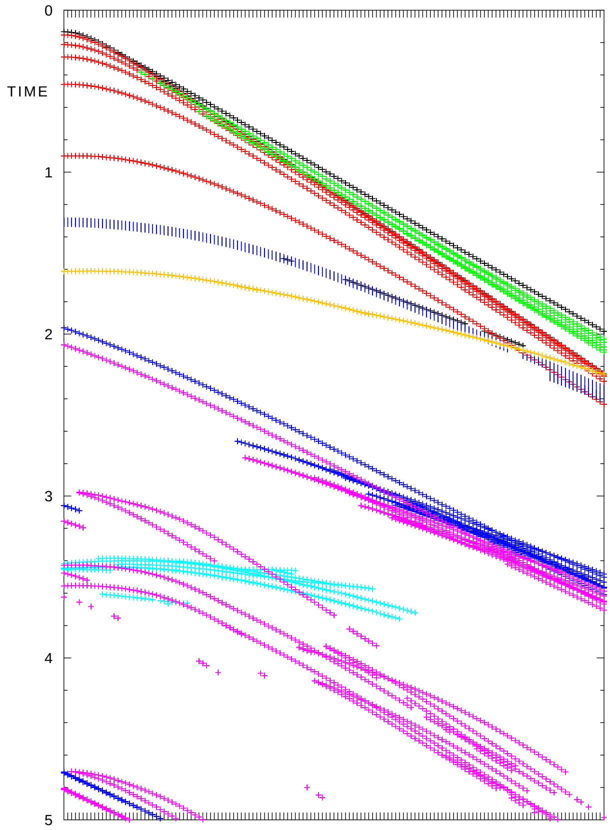

Ray-theory travel times

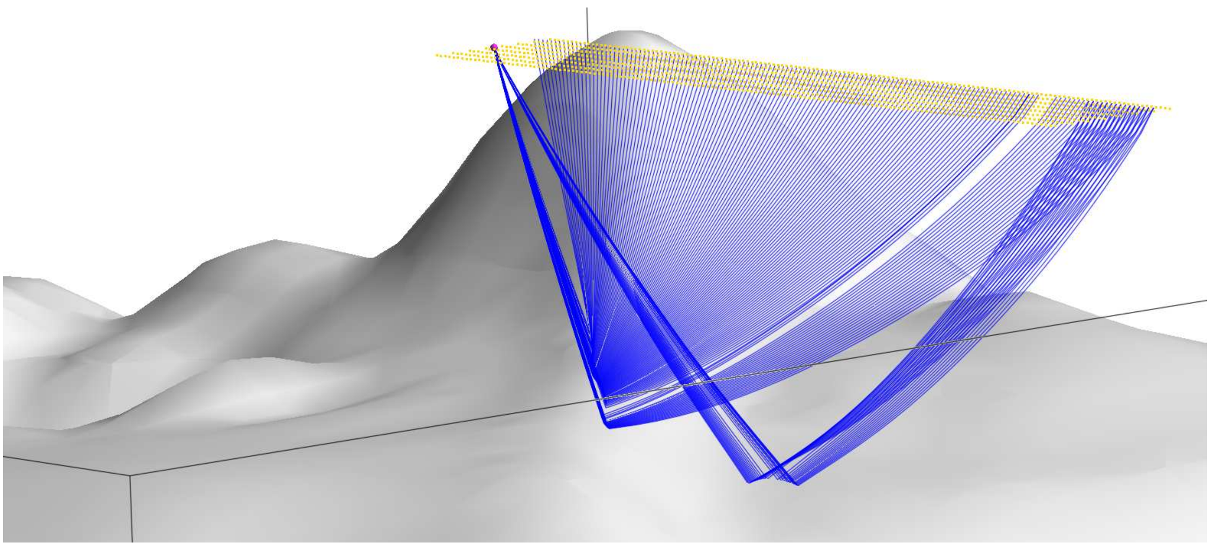

Rays of P-wave reflected from the top salt interface.

Figure 5. Marine streamer, South direction, line 7.

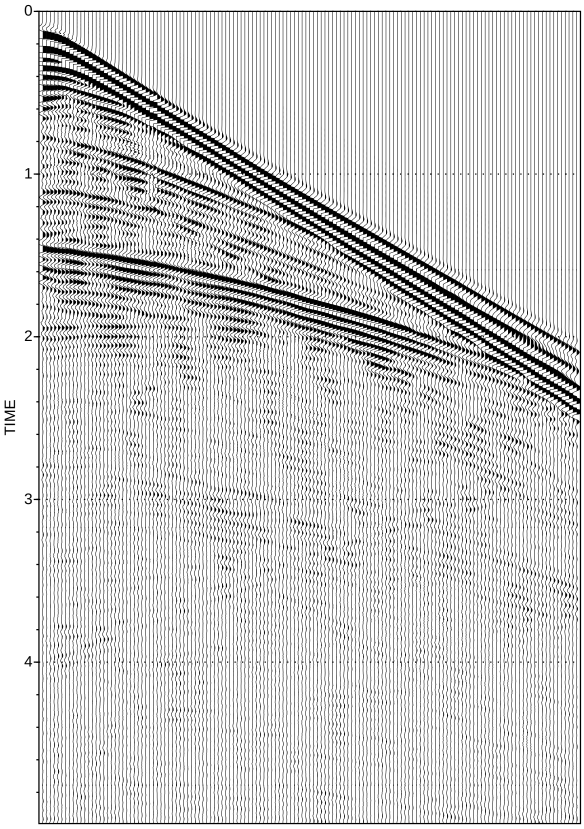

Finite-difference seismograms

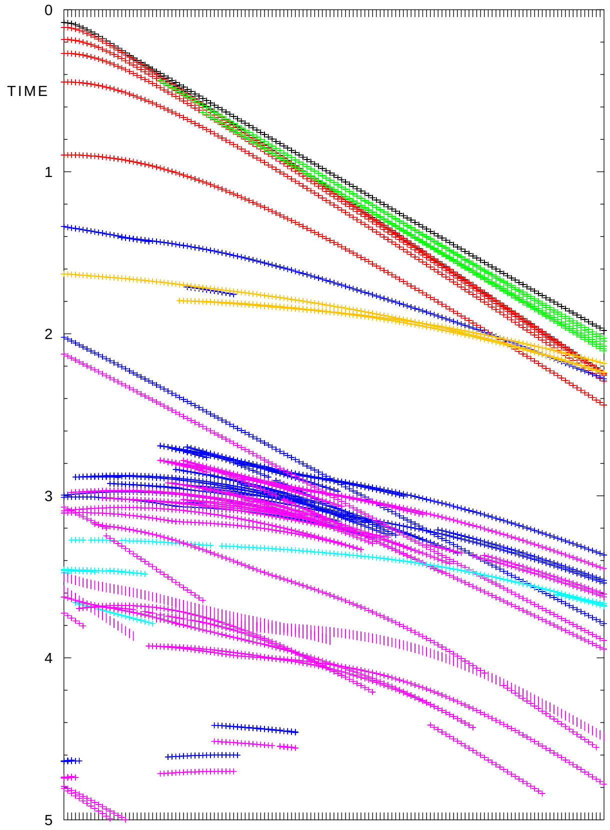

Ray-theory travel times

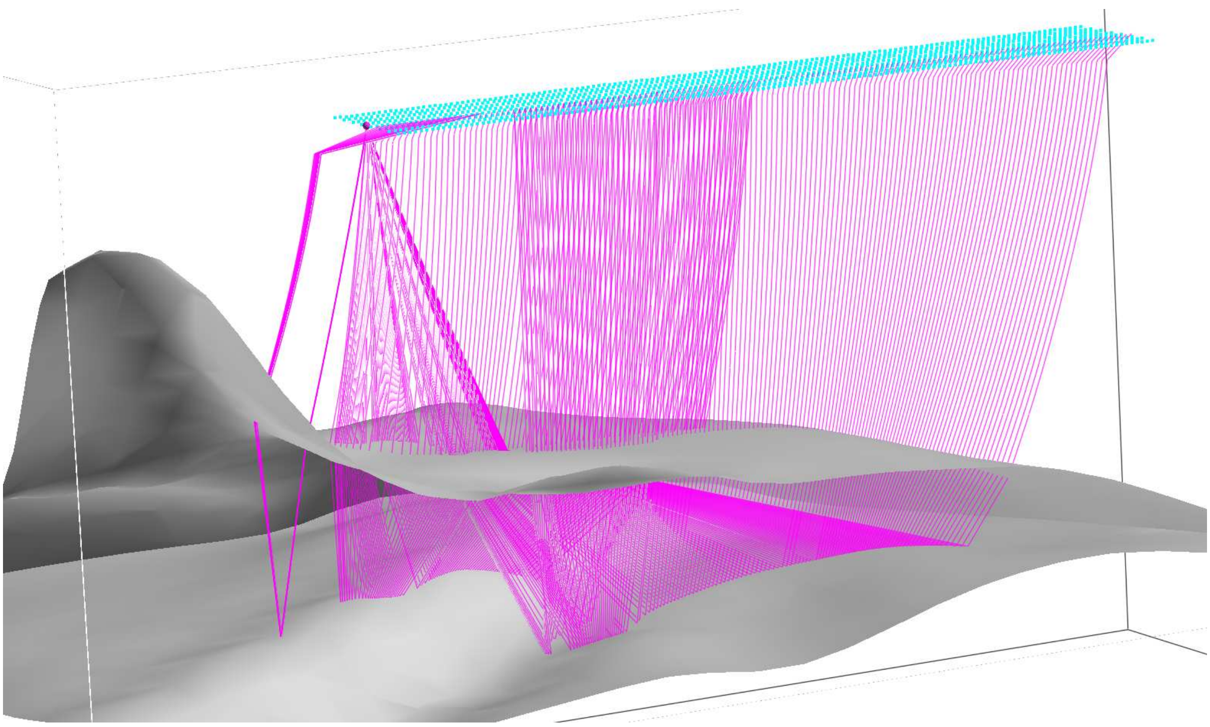

Rays of P-wave reflected and converted to S-wave at the bottom of the salt body.

Figure 6. Marine streamer, West direction, line 3.

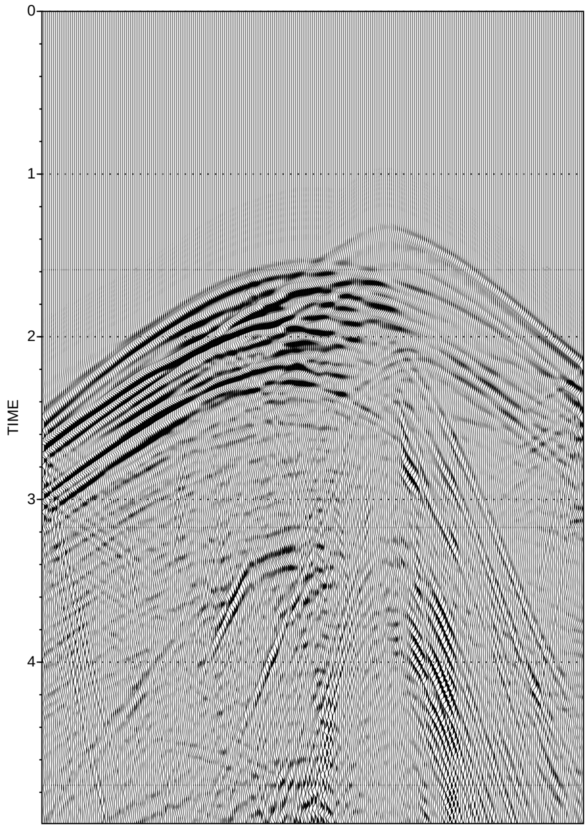

Finite-difference seismograms

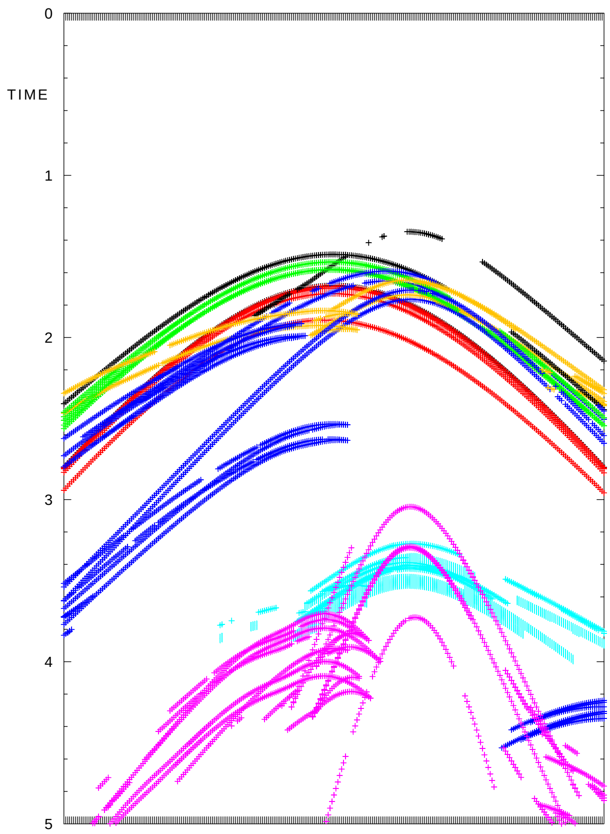

Ray-theory travel times

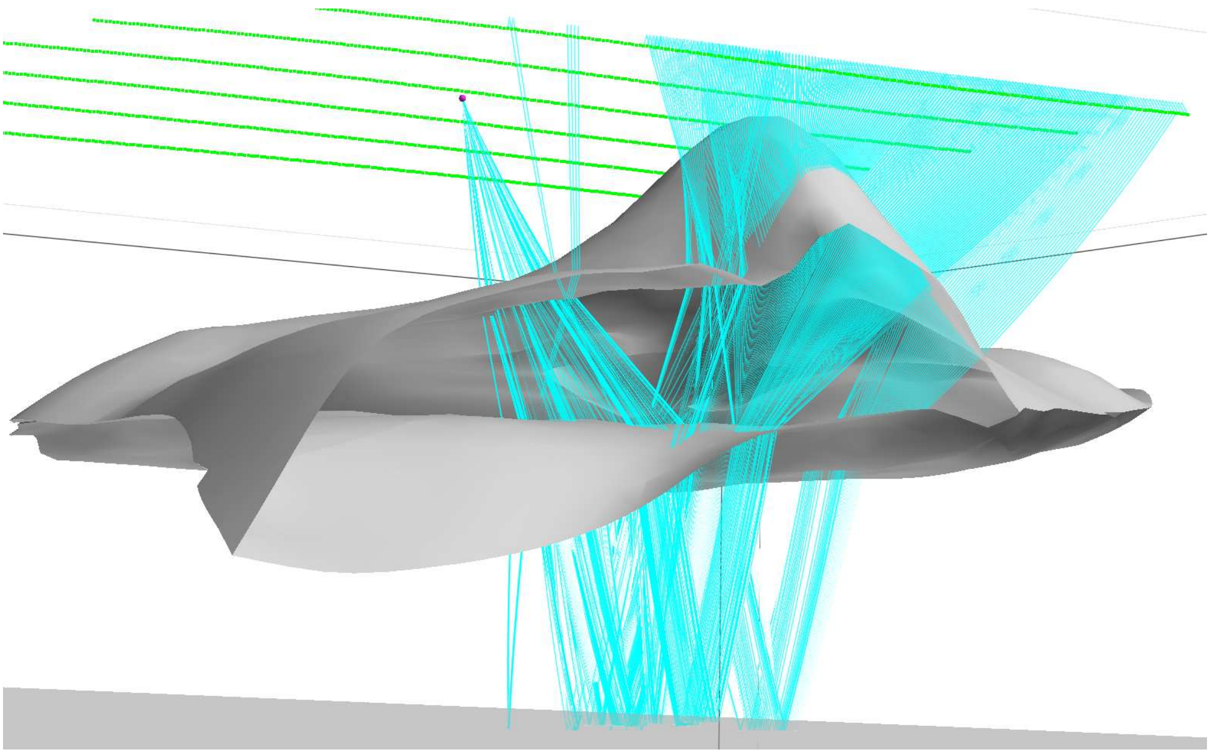

Rays of P-wave reflected from the bottom flat interface and the sea level.

Figure 7. Ocean bottom cable, North-South direction, line 1.

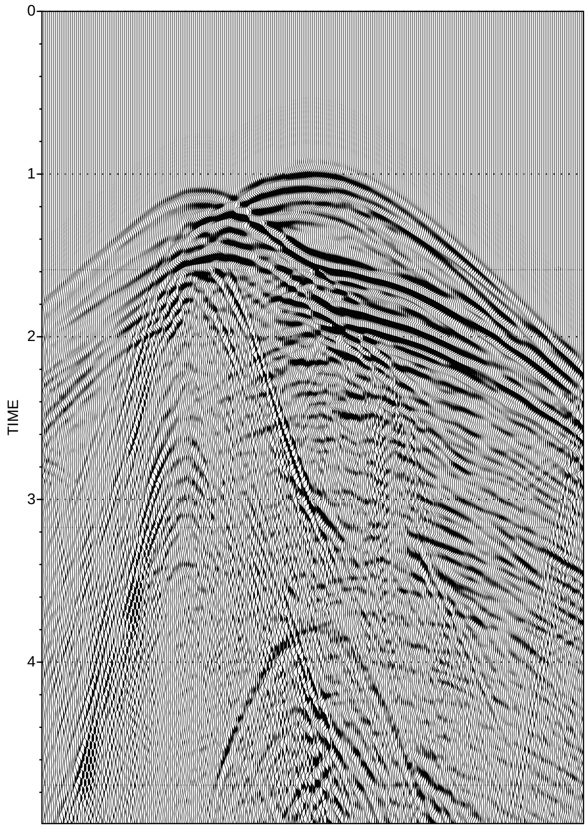

Finite-difference seismograms

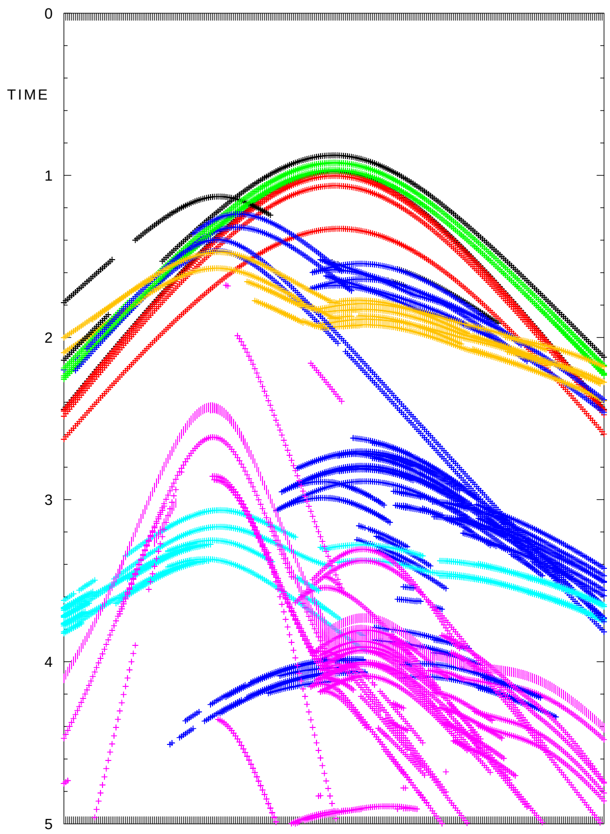

Ray-theory travel times

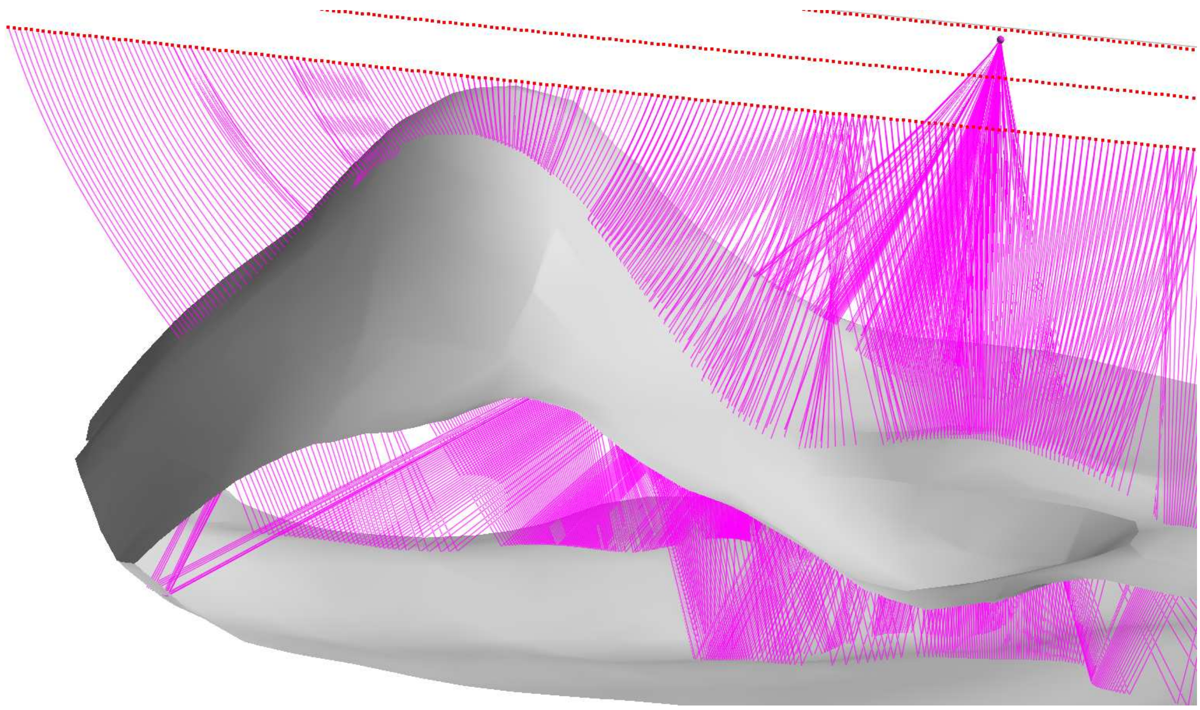

Rays of P-wave reflected and converted to S-wave at the bottom of the salt body.

Figure 8. Ocean bottom cable, East-West direction, line 5.

CONCLUSIONS

The results of the calculations demonstrate that the smoothed elastic SEG/EAGE Salt Model is suitable for two-point ray tracing. The paper shows and explains some differences between finite-difference seismograms and ray-theory travel times for shot number 145 and five receiver configurations. Speed, low memory requirements, computation and visualization of ray paths and travel times of the individual elementary waves are the great advantages of the ray tracing method.

The computation time of travel times for one receiver line differs according to the position in the model. The average time for one marine streamer line was approximately nine hours and for one ocean bottom cable line approximately eleven hours on a PC equipped with an Athlon 64 3400+ (2.2 GHz) processor and with the Linux operating system.

ACKNOWLEDGMENTS

The author thanks Luděk Klimeš for valuable comments and recommendations concerning this paper.

The research was supported by the Grant Agency of the Czech Republic under Contract 205/04/1104, and by the members of the consortium "Seismic Waves in Complex 3-D Structures" (see "http://sw3d.mff.cuni.cz").

REFERENCES

Aminzadeh, F., Brac, J. and Kunz, T., 1997. 3-D Salt and Overthrust Models, SEG/EAGE 3-D Modeling Series No.1. Soc. Explor. Geophysicists, Tulsa, OK.

Bucha, V., 2005. Comparison of finite-difference and ray-theory seismograms in the elastic SEG/EAGE Salt Model, shot number 145. In: Seismic Waves in Complex 3-D Structures, Report 15, Dep. Geophys., Charles Univ., Prague: 189–206, online at "http://sw3d.mff.cuni.cz".

Bucha, V., 2006. Comparison of finite-difference seismograms and ray-theory travel times in the elastic SEG/EAGE Salt Model, shot 145. In: Seismic Waves in Complex 3-D Structures, Report 16, Dep. Geophys., Charles Univ., Prague: 29–46, online at "http://sw3d.mff.cuni.cz".

Bucha, V. and Bulant, P. (Eds.), 2006. SW3D-CD-10. In: Seismic Waves in Complex 3-D Structures, Report 16, Dep. Geophys., Charles Univ., Prague: 307, online at "http://sw3d.mff.cuni.cz".

Bulant, P., 2001. Sobolev scalar products in the construction of velocity models - application to model Hess, to SEG/EAGE Salt Model, and to model Pluto 1.5. In: Seismic Waves in Complex 3-D Structures, Report 11, Dep. Geophys., Charles Univ., Prague: 133–159, online at "http://sw3d.mff.cuni.cz".

Bulant, P., 2002. Sobolev scalar products in the construction of velocity models: Application to model Hess and to SEG/EAGE Salt Model. Pure appl. Geophys., 159: 1487–1506.

Bulant, P., 2004. Constructing the SEG/EAGE 3-D Salt Model for ray tracing using Sobolev scalar products. Stud. Geophys. Geod., 48: 689–707.

Cohen, J.K. and Stockwell, Jr.J.W., 2004. CWP/SU: Seismic Un*x Release No. 38: a free package for seismic research and processing, Center for Wave Phenomena, Colorado School of Mines, online at "http://www.cwp.mines.edu/cwpcodes/".

Červený, V., Klimeš, L. and Pšenčík, I., 1988. Complete seismic-ray tracing in three-dimensional structures. In: Doornbos, D.J.(ed.), Seismological Algorithms, Academic Press, New York: 89–168.

Gardner, G.H.F., Gardner, L.W., and Gregory, A.R., 1974. Formation velocity and density - the diagnostic basis for stratigraphic traps, Geophysics, 39: 770–780.

House, S., Larsen, S. and Bednar, J.B., 2000. 3-D elastic numerical modeling of a complex salt structure. Exp. Abstr., Soc. Expl. Geophys. 70th Ann. Meet.: 2201–2204.

House, S., Larsen, S., Hoelting, C., Marfurt, K. and Wiley, R., 2004. Next-Generation Seismic Modeling and Imaging project: summary of elastic modeling results. Exp. Abstr., Soc. Expl. Geophys. 74th Ann. Meet.: 1869–1872.

Larsen, S. and Grieger, J., 1998. Elastic modeling initiative, part III: 3-D computational modeling, Exp. Abstr., Soc. Expl. Geophys., 68th Ann. Meet.: 1803–1806.